Pivotal Role for α1-Antichymotrypsin in Skin Repair*[S]

Daniel C. Hoffmann,[a] Christine Textoris,[a] Felix Oehme,[b] Tobias Klaassen,[c] Andreas Goppelt,[d] Axel Römer,[c] Burkhard Fugmann,[e] Jeffrey M. Davidson,[f,g] Sabine Werner,[h] Thomas Krieg,[a,i,j] and Sabine A. Eming[a,i,j1]

From the [a]Department of Dermatology, University of Cologne, 50931 Cologne, Germany, [b]Biotech Development, Bayer HealthCare AG, 42117 Wuppertal, Germany, [c]A&M Labor GmbH, 50126 Bergheim, Germany, [d]Baxter Innovation GmbH, 1020 Vienna, Austria, [e]Bayer Innovation GmbH, 40225 Düsseldorf, Germany, the [f]Research Service, Veterans Affairs Tennessee Valley Healthcare System, Nashville, Tennessee 37212, [g]Vanderbilt University School of Medicine, Nashville, Tennessee 37240, [h]ETH Zurich, Honggerberg, 8092 Zurich, Switzerland, and the [i]Center for Molecular Medicine Cologne and [j]Cologne Excellence Cluster on Cellular Stress Responses in Aging-associated Diseases, University of Cologne, 50674 Cologne, Germany

α1-Antichymotrypsin (α1-ACT) is a specific inhibitor of leukocyte-derived chymotrypsin-like proteases with largely unknown functions in tissue repair. By examining human and murine skin wounds, we showed that following mechanical injury the physiological repair response is associated with an acute phase response of α1-ACT and the mouse homologue Spi-2, respectively. In both species, attenuated α1-ACT/Spi-2 activity and gene expression at the local wound site was associated with severe wound healing defects. Topical application of recombinant α1-ACT to wounds of diabetic mice rescued the impaired healing phenotype. LC-MS analysis of α1-ACT cleavage fragments identified a novel cleavage site within the reactive center loop and showed that neutrophil elastase was the predominant protease involved in unusual α1-ACT cleavage and inactivation in nonhealing human wounds. These results reveal critical functions for locally acting α1-ACT in the acute phase response following skin injury, provide mechanistic insight into its function during the repair response, and raise novel perspectives for its potential therapeutic value in inflammation-mediated tissue damage.

Skin injury induces a complex cellular response, involving up-regulation/activation of various growth factors, their receptors, extracellular matrix molecules, and diverse classes of proteases, with the primary goal to rapidly restore the skin barrier function and to re-establish tissue homeostasis. Restoration of the epidermis is achieved by epithelialization, and repair of the mesenchymal tissue involves formation of granulation tissue, which includes inflammation, angiogenesis, myofibroblast differentiation, and matrix deposition (1). These events are highly dynamic and tightly controlled in time and space. Indeed, failure to resolve the inflammatory response leads to abrogation of the repair process and nonhealing states with severe medical and economic impact (2). Substantial experimental and clinical evidence highlights the fundamental importance of a tightly regulated balance among different classes of proteases and their inhibitors during the wound healing process (3, 4). Perturbations of the protease-inhibitor equilibrium with subsequent uncontrolled destruction of a variety of structural and functional proteins are considered the primary molecular mechanism underlying impaired healing in chronic skin ulcers associated with vascular disease (venous/arterial), diabetes mellitus, and aging (5, 6). However, detailed knowledge on the disregulation of specific protease/inhibitor systems and direct functional consequences for the tissue repair response is scarce.

In physiological skin repair a network of different classes of proteases and inhibitors, derived not only from blood plasma but also from diverse resident and nonresident skin cells, orchestrates the protease/inhibitor balance at the wound site. In chronic nonhealing skin ulcers, the prolonged and persistent leukocyte infiltrate is an important source of unrestrained protease activity (5–7). The major polymorphonuclear leukocyte-derived serine proteinases elastase (5, 6), proteinase-3, and cathepsin G (8), as well mast cell-derived chymase (9), are likely to be of particular importance for the excessive pathological tissue destruction seen under these conditions. Protease inhibitors neutralizing these potent serine proteases are induced at the wound site in resident skin cells after injury, for example, epithelium-derived antiproteinase (SKALP/elafin) or secretory leukocyte protease inhibitor (10, 11). Direct evidence for the importance of epithelium-derived secretory leukocyte protease inhibitor in skin repair is provided by the severely impaired healing response of gene-modified mice deficient in secretory leukocyte protease inhibitor (12, 13). However, direct evidence for the role of blood plasma-derived protease inhibitors controlling leukocyte-derived proteases at the cutaneous wound site is currently lacking.

The serpin family member α1-antichymotrypsin (α1-ACT,[2] serpin A3) represents one of the most abundant and potent plasma inhibitors for leukocyte-derived proteases and would likely contribute to reducing tissue damage by proteases that are released at the site of skin injury. Although its biological role is still uncertain, α1-ACT appears to be physiologically indis-

[S] The on-line version of this article (available at http://www.jbc.org) contains supplemental Figs. 1 and 2 and Table 1.

[1] To whom correspondence should be addressed: Dept. of Dermatology, University of Cologne, Joseph-Stelzmann Str. 9, 50931 Köln, Germany. Tel.: 49-221-4783196; Fax: 49-221-4200988; E-mail: sabine.eming@uni-koeln.de.

[2] The abbreviations used are: α1-ACT, α1-antichymotrypsin; BisTris, 2-[bis(2-hydroxyethyl)amino]-2-(hydroxymethyl)propane-1,3-diol; α-SMA, α-smooth muscle actin; rα1-ACT, recombinant α1-ACT.

pensable, because no homozygous α1-ACT-deficient individuals have been reported (14). The biological importance of α1-ACT in the extravascular compartment for tissue homeostasis is clearly shown in a variety of heterozygotic degenerative diseases (serpinopathies) that affect its structure and/or secretion and thereby reduce its activity and contribute to severe leukocyte protease-mediated tissue damage (14). The best studied diseases include emphysema (15), liver cirrhosis (16), and mental disorders (17). However, the role of this serpin member in the repair response after skin injury is still unknown.

α1-ACT is a glycoprotein of ~50–60-kDa mass, which shares 42% sequence homology with the archetypal serpin member α1-antitrypsin (serpin A1) (18). α1-ACT, like most inhibitory serpins, forms enzymatically inactive and irreversible stoichiometric complexes with its classical chymotrypsin-like target proteinases, including neutrophil cathepsin G, mast cell chymase, or pancreatic chymotrypsin. Binding of the substrate to the reactive center loop of α1-ACT leads to irreversible protease inhibition and a cleaved C-terminal fragment of α1-ACT (post-complex fragment) (19–21).

The purpose of this study was to investigate the function of α1-ACT in skin injury and repair and its potential role in impaired healing conditions. A number of documented functions of α1-ACT *in vitro* suggest a potential role in the protection from inflammation-mediated tissue damage and in the promotion of tissue-regenerative processes. In addition to its antiprotease properties (22, 23), α1-ACT affects the inflammatory response, *e.g.* through modulation of chemokine activation (24) and/or inhibition of superoxide anion production in activated neutrophils (25). Recently, we identified several members of the serpin protein family, particularly α1-ACT, in a differential proteomic analysis that distinguished tissue repair biomarker signatures among healing and nonhealing human skin wounds (26). Therefore, when viewed in the context of degenerative nonhealing skin wounds, α1-ACT is a potential candidate for protecting the tissue against proteolytic attack and for enhancing the healing response. The results presented in this study provide functional evidence for such a crucial function of α1-ACT in the wound healing process and identify this protein as a novel target for the treatment of recalcitrant nonhealing skin ulcers.

EXPERIMENTAL PROCEDURES

Animals—C57BLKS/J-m+/+Lepr[db/wt] mice (The Jackson Laboratory, Bar Harbor, ME) were mated; mice homogenous for the leptin receptor mutation developed diabetes (db/db), and mice lacking the mutation (WT) were used as control animals. Genotyping of mice was performed as described previously (27). Mice (male, 10–12 weeks of age) were caged individually under standard pathogen-free conditions in the animal care facility of the Center for Molecular Medicine Cologne, Cologne, Germany.

Excisional Wounding and rα1-ACT Treatment in Mice—Two independent wound healing experiments were performed. In total, three mice per time point and condition (in total 12 experimental mice and 6 control mice) were analyzed. Mice were anesthetized under Ketanest/Rompun (Ketanest S, Park Davies GmbH, Karlsruhe, and 2% Rompun, Bayer, Leverkusen,

Germany). The backs of the animals were shaved, and four full-thickness punch-biopsy wounds were created. Immediately after wounding and then for the following 6 days, treatment of wounds was performed by either applying 50 μl of rα1-ACT solution at two different concentrations (0.4 or 2.0 mg/ml) (08ACT04-04, Bayer Schering Pharma, Wuppertal, Germany) or vehicle (0.9% NaCl solution) (control) onto the wound bed. Solution was allowed to adsorb for at least 1 h before the animal was placed back into its cage. Wound closure was determined through digital processing of photographs taken daily during the time of healing using the Imaging Software Lucia G 4.80 (Dental Eye, Olympus, Japan; Imaging Software Lucia G 4.80, Laboratory Imaging Ltd., Prague, Czech Republic). For histological analysis, animals were sacrificed, and wound tissues were harvested 5 and 10 days after wounding. Wound tissue was excised, and the wound area bisected in a caudocranial direction. The tissue was either fixed overnight in 4% paraformaldehyde in phosphate-buffered saline (PBS) or embedded in OCT compound (Tissue Tek, Sakura Finetek, NL), immediately frozen in liquid nitrogen, and stored at −80 °C. Histological analysis was performed on serial sections (5-μm cryosections) from the central portion of the wound.

Histology and Immunohistochemistry—To process tissue sections for the detection of CD31 (PECAM-1), 5-μm cryosections were fixed in acetone, and endogenous peroxidase was inactivated (0.03% H_2O_2, 0.15 M NaN3), and unspecific binding sites were blocked with 3% BSA in PBS. Sections were incubated with polyclonal rat antisera against murine CD31 (1 h at room temperature, 1:500, Pharmingen, Heidelberg, Germany). Bound primary CD31 antibody was detected using an Alexa Fluor 488-conjugated polyclonal goat anti-rat antibody (1 h, 1:500, Molecular Probes, Leiden, The Netherlands). For staining of α-SMA, cryosections were fixed and blocked as outlined above and incubated with Cy3-conjugated mouse monoclonal anti-α-SMA antibody (1 h, room temperature, 1:200, Sigma). For double staining of α1-ACT and CD68 in human wound tissue, cryosections were fixed and blocked as outlined above and incubated with polyclonal rabbit antibody against human α1-ACT (1:50 dilution, 1 h at room temperature; Biotrend GmbH, Cologne, Germany) and monoclonal mouse antibody against human CD68 (1:100 dilution, 1 h at room temperature; BMA Biomedicals). Bound primary antibody was detected using an Alexa Fluor 594-conjugated polyclonal goat anti-rabbit antibody and Alexa Fluor 488-conjugated polyclonal goat anti-mouse antibody, respectively. α1-ACT staining on mouse wound tissue was performed on paraffin sections using the Dako Envision anti-rabbit HRP kit (DakoCytomation, Hamburg, Germany) with 3-amino-9-ethylcarbazole as substrate. The α1-ACT antibody cross-reacts to 60% with mouse α1-ACT, as indicated by the manufacturer. As a control for specificity, primary antibodies were omitted and replaced by irrelevant isotype-matched antibodies.

Nonradioactive in Situ Hybridization—Mouse cDNA of 5-day-old wounds was subjected to 40 cycles of PCR to generate a fragment of Spi-2 (nucleotides 1036–1334, GenBank™ accession number NM_009252.2). The resultant cDNA fragment was subcloned using a TOPO cloning kit according to the manufacturer's protocol (Invitrogen) and was verified by

sequencing. Digoxigenin-labeled sense and antisense ribo-probes were synthesized with T3 and T7 polymerases, using the digoxigenin RNA labeling mixture from Roche Applied Science according to the manufacturer's protocol. Nonradioactive *in situ* hybridization was performed as described previously (28). Hybridization signals were visualized using 5-bromo-4-chloro-3-indolyl phosphate and nitro blue tetrazolium.

Morphometric Analysis—Immunofluorescence/immunohistochemical microscopy was conducted at the indicated magnifications (Microscope Eclipse 800E; Nikon, Düsseldorf, Germany). Morphometric analysis was performed on digital images using the imaging software Lucia G 4.80 (Laboratory Imaging Ltd., Prague, Czech Republic). The extent of epithelialization and granulation tissue formation was determined on hematoxylin and eosin (H&E)-stained paraffin tissue sections. The length of the epithelial tongue was determined as the distance between the epithelial tip and the margin of the wound as defined by the presence of hair follicles in nonwounded skin. This parameter reflects the formation of neo-epithelium. In addition, the width of the gap between the epithelial tips reflects wound closure. The distance between the edges of the panniculus carnosus was determined as a measure of wound contraction. Granulation tissue was defined as the cellular and vascular tissue that formed underneath the neo-epithelium and between the wound margins and above the subcutaneous fat tissue. For quantitative analysis of CD31 or α-SMA expression, the area that stained positive for CD31 or α-SMA within the granulation tissue was calculated.

Human Wound Exudates and Wound Tissue—Wound exudate was obtained from patients presenting with nonhealing chronic ulcera crura due to venous insufficiency ($n = 15$) or from patients with normally healing cutaneous wounds ($n = 5$; excisional wounds of the lower leg awaiting wound closure by secondary intention). A summary of the clinical features and wounds from patients is provided in supplemental Table 1. To accumulate exudate, the wound was covered with a semipermeable polyurethane film (Hyalofilm, Hartmann, Heidelberg, Germany) for a maximum of 8 h. A maximum of 1 ml of exudate per wound was usually obtained. Following exudate collection, fluids were centrifuged (10 min, $13,000 \times g$, 4 °C) to remove insoluble material, and supernatants were frozen at -80 °C until use. Biopsies were taken by consent from patients presenting chronic ulcera crura ($n = 8$) due to venous insufficiency; for clinical features and wounds from patients see supplemental Table 1. The biopsies (spindle-shaped 1 cm length $\times$ 0.3 cm width $\times$ 0.5 cm depth) were obtained from the wound edge of chronic wounds. Tissue of normally healing human wounds ($n = 4$ per time point) was taken by consent from healthy volunteers. Wounds were created by performing a punch biopsy (6 mm diameter $\times$ 0.5 cm depth), and at indicated time points following wounding, the wound was excised. Wound tissues were processed for histological analysis as described for murine tissue. The study adhered to the Declaration of Helsinki Principles, and skin biopsies were collected according to a protocol approved by the Ethics committee at the University of Cologne and Technical University of Munich (tissue samples of normal healing wounds used for quantitative RNA analysis); written

informed consent from patients was received prior inclusion in the study.

Real Time RT-PCR Analysis—Wound tissue was excised at different time points after injury as indicated. For preparation of RNA, the tissue from four mouse wounds or four human wounds per time point was pooled, immediately frozen in liquid nitrogen, and stored at -80 °C until used for RNA isolation. After homogenization of biopsies, total RNA was prepared by a modification of the method of Chomczynski and Sacchi (58). For cDNA synthesis, MultiScribe reverse transcriptase and random hexamers (Applied Biosystems, Foster City, CA) were used according to the manufacturer's instructions. Murine *spi-2.2* expression was normalized to *gapdh*, whereas α1-ACT was quantified relative to cyclophilin. Primers specific for murine *gapdh* are as follows: forward 5′-ATC AAC GGG AAG CCC ATC A-3′ and reverse 5′-GAC ATA CTC AGC ACC GGC CT-3′. Primers specific for *spi-2.2* are as follows: 5′-CTG TCC TCT GCT TCC CAG ATG-3′ and 5′-TCC AGT TGT GTC CCA TTG TCA-3′. Primers specific for human cyclophilin are as follows: forward 5′-GGA ATG GCA AGA CCA GCA AG-3′ and reverse 5′-GGA TAC TGC GAG CAA ATG GG-3′. Primers specific for human *aact* are as follows: forward 5′-AGG CCT TTG CCA CTG ACT TTC-3′ and reverse 5′-GCG AGT CAA GGT CCT TGA TCA-3′. Amplification reactions, each in triplicate, were set up using PowerSYBR Green PCR master mix (Applied Biosystems). Quantitative real time RT-PCR was performed using the 7300 real time PCR system (Applied Biosystems). The comparative method of relative quantification ($2^{-\delta\delta Ct}$) was used to calculate expression level of the target gene normalized to *gapdh* or cyclophilin. Data are expressed as relative increase of *spi-2.2* and *aact* expression over healthy nonwounded skin.

Quantification of Active α1-ACT Protein Using an Enzyme-linked Immunosorbent Assay—96-Well plates (Nunc Immuno Plate Maxi Sorp, Sigma) were coated with human cathepsin G protein (1 μg/ml; 100 μl/well) (AppliChem GmbH, Darmstadt, Germany) in phosphate-buffered saline (PBS). After overnight incubation at 4 °C, plates were washed four times with 0.05% Tween 20 in PBS. Nonspecific binding sites were blocked with 1% bovine serum albumin in PBS for 30 min at room temperature. A serial dilution of wound exudate or plasma serum samples was prepared in 1% BSA in PBS (measurements were performed in duplicate). Recombinant human α1-ACT protein (rα1-ACT protein synthesized in *Escherichia coli*) served as a standard; the sensitivity of the assay was 0.4–43.5 ng/ml; reaction time was 60 min at 37 °C. Bound α1-ACT was detected with a rabbit antibody against human α1-ACT (1:1000 dilution, 60 min at 37 °C; Biotrend GmbH, Cologne, Germany). Bound primary antibody was detected using an alkaline phosphatase-conjugated goat antibody against rabbit IgG (1:5000 dilution, 60 min at 37 °C, Sigma). Alkaline phosphatase was reacted with *p*-nitrophenyl phosphate substrate (Sigma), and the reaction product was quantified using an ELISA plate reader (Nunc Immunoreader NJ 2000, Sigma) at 405 nm. Concentration of active α1-ACT was calculated by four-parameter regression (GraphPad Prism 5).

Synthesis of Recombinant Human α1-ACT Protein—Recombinant human α1-ACT (rα1-ACT) was expressed in *E. coli*

W3110. Expression was performed in Terrific Broth containing 25 mg/liter kanamycin at 25 °C overnight. Cells were lysed in ice-cold 50 mM citrate, 50 mM NaCl, pH 5, 0.25 mg of lysozyme per g cell wet weight, 10 mM MgCl$_2$, 12.5 units/ml benzonase by high pressure homogenization. After centrifugation, the cleared supernatant was applied onto a Capto MMC column (GE Healthcare) equilibrated with 50 mM Tris, pH 8. After washing with equilibration buffer, the product was eluted with a linear gradient to 50 mM Tris, 1 M NaCl, pH 8.3. Fractions containing α1-ACT were pooled, dialyzed against 50 mM Tris, 50 mM NaCl, pH 7.5, and applied onto a Capto Q column (GE Healthcare). The column was washed with 50 mM Tris, 50 mM NaCl, pH 7.5, and the product was eluted with a linear gradient to 1 M NaCl in washing buffer. The final product was dialyzed against 10 mM Tris, 1% sucrose, 2% glycine, pH 7.5, and lyophilized. Endotoxin content in the final product was 12 endotoxin units/mg, and the purity was >95% as determined by RP-HPLC and SDS-PAGE. Identity of the product was confirmed by mass spectrometry and by N-terminal sequencing.

Synthesis of α1-[^{15}N]ACT was performed in 800 ml shaking flasks at 25 °C by incubating cells in a minimal medium with [^{15}N]NH$_4$Cl. After cell lysis by high pressure homogenization, the protein was purified as described above for the unlabeled rACT. The final product was stored frozen at −70 °C. Activity of rα1-ACT was shown by inhibition of cathepsin G. ACT was incubated at different concentrations with cathepsin G (AppliChem; final concentration 7.3 μg/ml; 0.25 μM) in a total volume of 300 μl (20 mM HEPES, pH 7.5). The substrate succinyl-AAPF-*p*-nitroanilide was used to monitor cathepsin G activity, and the reaction rate was detected in microtiter plates at 410 nm for 10 min at room temperature.

SDS-PAGE Immunoblotting—SDS-PAGE was performed following the protocol of Laemmli (59). To analyze the stability of rα1-ACT in wound fluid, 600 ng of rα1-ACT protein produced in *E. coli* was incubated at 37 °C with 9 μl of wound fluid and reaction buffer (50 mM Tris, 200 mM NaCl, pH 7.5). At indicated time points, reactions were terminated by the addition of reducing Laemmli buffer. The reactions were resolved on a 4–12% reducing BisTris SDS-polyacrylamide gel (NuPAGE, Invitrogen) and transferred to a nitrocellulose membrane (Hybond C-extra, Amersham Biosciences). Integrity of rα1-ACT was determined by detecting immunoreactive products with an anti-human rα1-ACT monoclonal mouse antibody (1:5000, US Biological). Bound primary antibody was detected using an anti-mouse HRP-conjugated secondary antibody (1:2000, DAKO A/S, Denmark). Detection was accomplished using the enhanced chemiluminescence Western blot detection system (ECL, Amersham Biosciences).

To assess complex formation of rα1-ACT with its target proteases, rα1-ACT was diluted to a concentration of 1.5 mg/ml in 25 mM Tris buffer, pH 7.5, and cathepsin G (AppliChem) was diluted to a concentration of 1 mg/ml in 25 mM NaCH$_2$COOH, pH 5.5, containing 400 mM NaCl. The two components were mixed in different ratios as indicated to give a final volume of 50 μl and were incubated for 5 min at 37 °C to allow formation of the complex. The reaction was terminated by addition of 17 μl of NuPAGE LDS sample buffer and heated at 70 °C for 10 min. The samples were separated on a BisTris gel (4–12%) according

to the supplier's instruction. Gel staining was performed with the colloidal blue staining kit (Invitrogen).

Assessment of rα1-ACT Protein Degrading Activity in Wound Exudate—Working solutions of rα1-ACT and the internal standard rα1-[^{15}N]ACT were prepared by dilution of rα1-ACT and rα1-[^{15}N]ACT stock solutions with 50 mM Tris/HCl, pH 7.5. To assess the rα1-ACT degrading activity of the wound exudates, 10 μl of exudate were transferred into 1.5-ml safe-lock tubes, and 10 μl of inhibitor solution was added. After that, 50 μl of rα1-ACT working solution (1.5 mg/ml) were transferred into the sample tubes, and the mixture was incubated at room temperature for a defined period. The incubation was stopped by addition of 10 μl 20% phosphoric acid (Merck) or 98–100% formic acid (Merck). Finally, 50 μl of internal standard working solution and 1900 μl of 50 mM Tris/HCl, pH 7.5, were added, and the sample was transferred to LC-MS analysis. The following substances were examined for their potential to inhibit rα1-ACT degradation: SSR 69071 (concentrations as indicated; Tocris Biosciences, Bristol, UK), EDTA disodium dihydrate (5 mM) (Merck), ciclopiroxolamine (1.43 and 14.3 μM), deferoxamine mesylate (0.143 and 1.43 mM), doxycycline hyclate (71.4 and 714 μM), and 1,10-phenanthroline (0.0143, 0.143, 1.43 mM) (all Sigma).

Characterization of rα1-ACT Truncation—Comparative measurements between stabilized and nonstabilized exudate samples were performed. For the stabilized exudate samples, phosphoric or formic acid was added prior to rα1-ACT, so that the processing order was exudate + acid + rα1-ACT → incubation → internal standard + Tris buffer. In contrast, acid was not added until the end of the incubation period for the nonstabilized exudate samples exudate + rα1-ACT → incubation → internal standard + Tris buffer. The chromatograms were visually compared for obvious differences in their peak patterns. The pertaining *m/z* ratios of conspicuous chromatographic peaks were deconvoluted using ProMass for Xcalibur, version 2.5 SR-1 (Novatia, Monmouth Junction, NJ), and verified with N- and C-terminal rα1-ACT peptide fragments known from literature or calculated by GPMAW32, version 10sr1 (Lighthouse Data, Odense, Denmark).

LC-MS Analysis—Chromatographic separation was performed using gradient elution with water + 0.05% trifluoroacetic acid and acetonitrile + 0.05% trifluoroacetic acid as mobile phases and a YMC-Pack Butyl, 20 nm, S-5 μm; 10 × 2.1-mm column (YMC, Dinslaken, Germany). The samples for the assessment of the rα1-ACT degrading activity of wound exudates were measured with a TSQ Quantum Ultra triple quad mass spectrometer (Thermo Fisher Scientific, San Jose, CA). Positive electrospray ionization was used, and the following *m/z* ratios of the analyte and the internal standard were monitored in the selected reaction monitoring mode: 1377.0 Thomson (corresponding to the 33-fold charged [rαACT + H]$^{+33}$ ion) and 1436.4 Thomson (corresponding to the 32-fold charged [[15N]-rαACT + H]$^{+32}$ ion). The peak area ratios of the analyte and the corresponding internal standard peak were used to quantify the rα1-ACT concentrations. The cleavage products of rα1-ACT were identified and characterized using an LCQ ion trap (Thermo Fisher Scientific). An extended chromatographic gradient was applied to achieve optimal separa-

tion of the evolving peptides. A mass range of 300 to 2000 Thomson was observed after positive electrospray ionization.

Statistical Analysis—Data are presented as box plot diagrams or as mean ± S.E. A p value < 0.05 was considered significant. Statistical analyses and calculation of IC_{50} values for rα1-ACT were performed using GraphPad Prism 5 (GraphPad Software Inc., La Jolla, CA) and SPSS expert. Significance was analyzed using unpaired Student's t test for Gaussian distribution or the Mann-Whitney test.

RESULTS

α1-ACT Is Expressed in Skin Wounds—To determine whether α1-ACT is expressed at the wound site after skin injury and whether it might be differently expressed in a normal healing *versus* an impaired healing condition, we performed punch injuries on the back of wild-type and diabetic mice (db/db), and expression of Spi-2, the mouse homologue of α1-ACT (29), was quantified by real time PCR using RNAs from wound tissues at different stages after injury. The db/db mouse is a genetic mouse model of diabetes mellitus and provides a well established, clinically relevant experimental system of impaired wound healing (27, 30, 31). In wild-type mice, Spi-2 expression was strongly up-regulated within 7 h after injury, reaching its peak at 24 h, and then rapidly declining until day 5 post-injury (Fig. 1A). In contrast, Spi-2 expression was significantly less pronounced at all time points post-injury in wound tissue of db/db mice when compared with wild-type wounds (Fig. 1A). In addition, a strong up-regulation of α1-ACT expression was also seen in acute human wounds from healthy adult volunteers within hours post-injury, which then declined during the phase of tissue formation and maturation (Fig. 1B). These results demonstrate that Spi-2 and α1-ACT exhibit a classic acute phase response upon wounding of healthy murine and human skin, respectively.

To determine the sites of Spi-2/α1-ACT expression in the wound, mouse and human wound tissues were subjected to *in situ* hybridization and immunohistochemical staining. During the early phase of physiological repair, mouse wounds (day 3–5 post-injury) revealed a strong hybridization (Fig. 1C) and immunohistochemical staining signal (data not shown) for Spi-2 in suprabasal keratinocytes of the hyperproliferative epidermal wound edge, whereas only few dermal cells stained positive. In normal healing, human wound expression was also seen in the epidermis and macrophages as determined by co-staining with CD68 (Fig. 1D). In chronic nonhealing human wounds, the majority of α1-ACT-positive cells showed a strong co-staining for CD68, whereas suprabasal keratinocytes at the hyperproliferative wound edge were only weakly positive (Fig. 1D). Consistent with earlier reports for other tissues, α1-ACT signals showed a cytoplasmic as well as nuclear staining pattern (32). Not wounded normal skin showed no epidermal staining signal and only occasional co-staining with CD68 (Fig. 1D). Therefore, resident skin and nonresident inflammatory cells contributed to α1-ACT/Spi-2 activity in the cutaneous wound microenvironment.

Local Treatment with rα1-ACT Protein Rescues the Wound Healing Defect of Diabetic Mice—To determine whether the levels of α1-ACT are rate-limiting in diabetic mice and to test

the therapeutic potential of this protein, we evaluated the wound healing response in diabetic mice treated locally with repetitive applications of rα1-ACT at two concentrations. For this analysis, human rα1-ACT was expressed in *E. coli* and purified. To verify its activity, the rα1-ACT·cathepsin G complex formation was characterized. For this purpose, recombinant cathepsin G was added into a rα1-ACT solution at varying ratios and analyzed by reducing SDS-PAGE. Colloidal blue stain showed bands of higher molecular weight, indicating formation of rα1-ACT·cathepsin G complexes and consistent with authentic rα1-ACT activity ([supplemental Fig. 1A](#)). Activity of rα1-ACT was further evaluated by inhibition of cathepsin G, and the IC_{50} value was determined to be 0.46 μM ([supplemental Fig. 1B](#)).

Analysis of the wound closure rate demonstrated that repetitive rα1-ACT protein application to wounds in db/db mice significantly accelerated wound closure when compared with vehicle-treated wounds (Fig. 2, A and B). Accelerated wound closure was most prominent in wounds treated with 2.0 mg/ml rα1-ACT. These findings demonstrate that topical application of human rα1-ACT to wounds rescues the impaired healing phenotype of diabetic mice and that there is no species barrier of human rα1-ACT in mice. The homology between the murine and human α1-ACT protein has been reported to be ~60% (29).

Increased Deposition and Maturation of Granulation Tissue and Accelerated Epithelialization Mediate Wound Closure in rα1-ACT-treated Wounds of Diabetic Mice—We next analyzed the cellular repair mechanisms that might direct the rα1-ACT-mediated accelerated healing response in diabetic mice. Morphometric quantification of granulation tissue with H&E stainings at days 5 and 10 post-injury showed that application of rα1-ACT at the higher concentration significantly increased the formation and deposition of granulation tissue at both time points when compared with control wounds, whereas the lower concentration was superior only at day 10 post-injury ($p < 0.004$) (Fig. 2D). Granulation tissue of 2.0 mg/ml rα1-ACT-treated wounds consisted of numerous small capillaries, mononuclear cells, and spindle-shaped cells, judged by light microscopy to represent macrophages and fibroblasts, respectively. In contrast, the scarce granulation tissue observed in vehicle-treated wounds was poorly vascularized and showed few cells. Hence, keratinocytes at the wound edge of control wounds did not cover a vascularized granulation tissue as observed in rα1-ACT-treated wounds but rather covered the massive subcutaneous fat layer (Fig. 2C). As assessed by the length of the epithelial tongue (Fig. 2, E and F), epithelialization was significantly increased in day 5 post-injury in 2.0 mg/ml rα1-ACT-treated wounds compared with controls ($p = 0.0004$). Overall, these results confirm that topical application of rα1-ACT protein rescues the impaired healing diabetic phenotype and suggest that lack of α1-ACT in diabetic mice contributes to the attenuated repair response.

We measured the distance between the edges of the panniculus carnosus at the wound margins (Fig. 2G) to compare the relative contribution of epithelialization and increased deposition of granulation tissue *versus* contraction of the wound tissue. At day 5 post-injury, this distance was significantly shorter
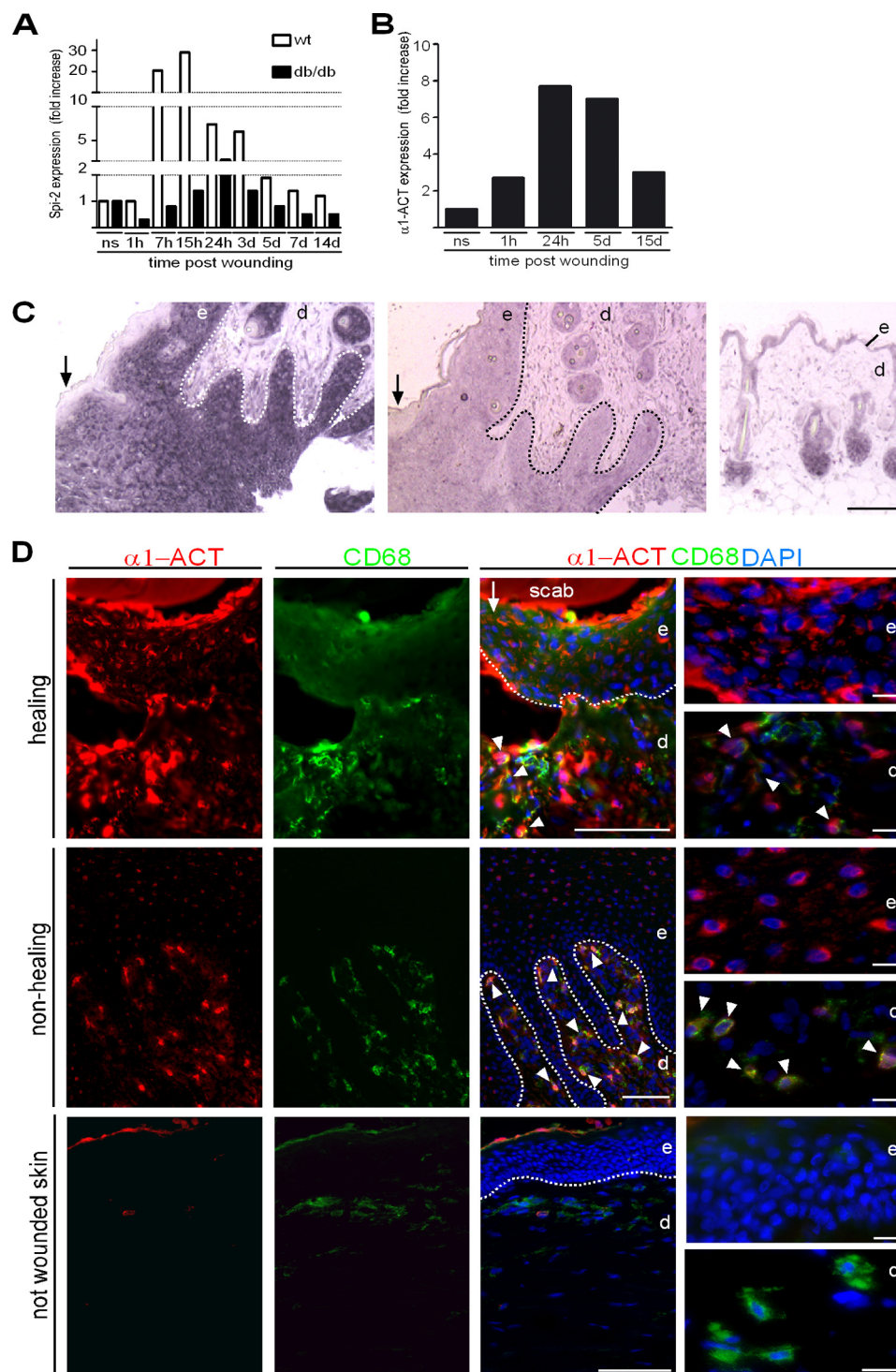
FIGURE 1. **Spi-2/α1-ACT is expressed during the acute phase response post skin injury.** *A,* quantitative RT-PCR analysis of RNA from wound tissue at indicated time points after injury revealed a dramatic increase in *Spi-2* mRNA in wild-type (*wt*) mice (wounds per time point $n = 4$), and at all time points expression in wounds of db/db mice (wounds per time point $n = 4$) was attenuated. *B,* levels of *α1-ACT* mRNA were also strongly up-regulated in normal healing human wounds (wounds per time point $n = 4$); *ns,* not wounded skin ($n = 4$); *h,* hours; *d,* day. *C,* paraffin sections of normal healing wounds (day 5 post-injury) (*left* and *middle*) and intact skin (*right*) were hybridized to a digoxigenin-labeled antisense probe for Spi-2 mRNA (*left* and *right*) and sense probe; reaction product appears in *purple*; some sections were counterstained with nuclear fast red. *D,* double immunofluorescence staining of α1-ACT (*red*) and CD68 (*green*) in tissue of a healing wound (day 3 post-injury), a nonhealing human wound, and not wounded skin; DAPI counterstaining of nuclei (*blue*); *dotted line* indicates basement membrane; *arrow* indicates wound edge; *arrowheads* indicate double-positive cells. *e,* epidermis; *d,* dermis. *Scale bars,* 100 μm in *C* and *D*; 20 μm in *D, right panel.*

in rα1-ACT treated wounds at both concentrations when compared with control wounds ($p < 0.04$). In 10-day-old rα1-ACT 2.0 mg/ml treated wounds immunostaining for α-SMA, a

marker for myofibroblast differentiation and a major molecular component of wound contraction, indicated that α-SMA was abundantly present throughout the entire layer of the late gran-
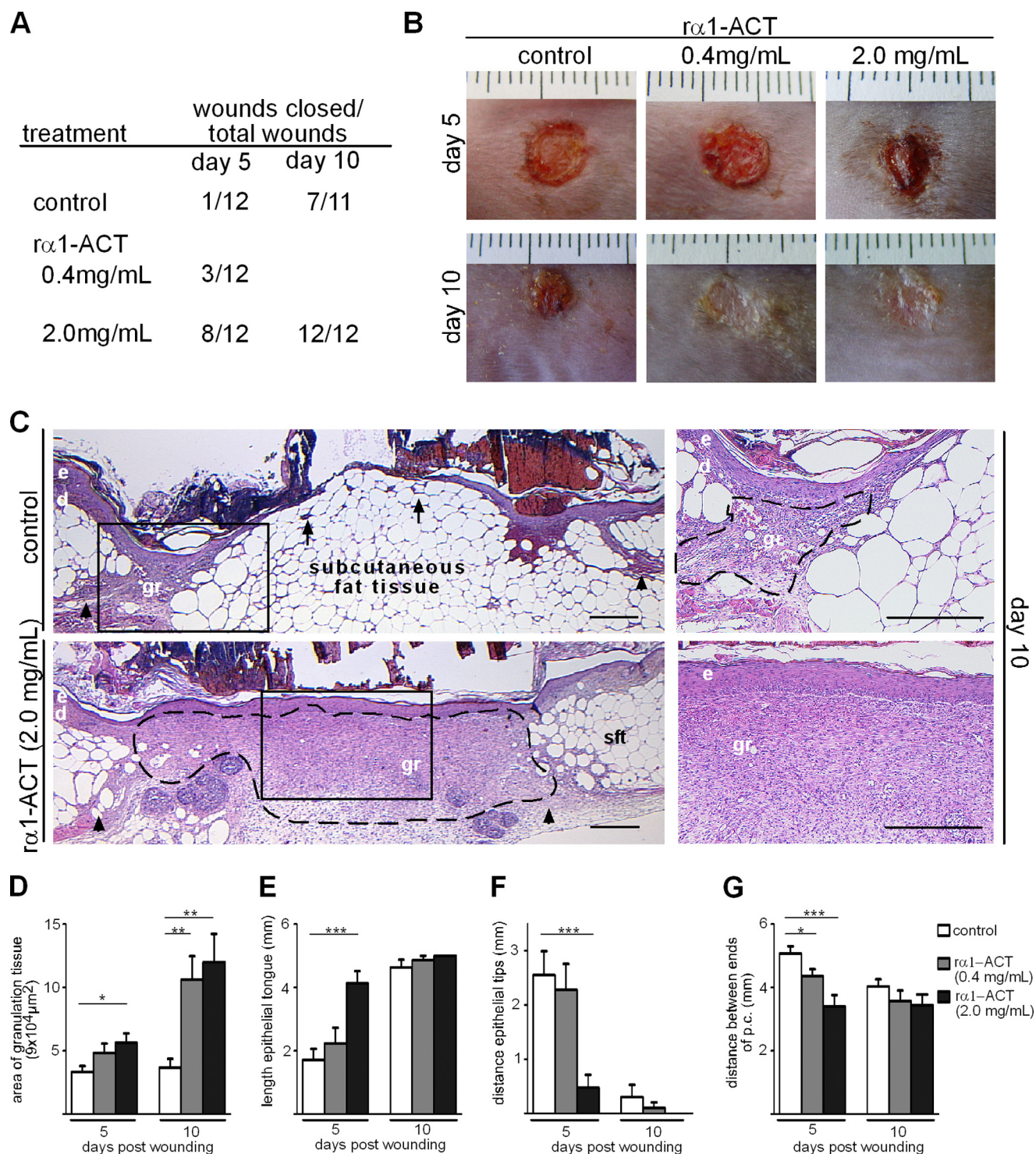
FIGURE 2. **Topical application of rα1-ACT accelerates granulation tissue formation and epithelialization in diabetic mice.** Repetitive application of rα1-ACT (concentrations as indicated) significantly accelerated wound closure kinetics of db/db mice compared with vehicle-treated controls. *A,* presented are numbers of closed wounds *versus* total number of wounds for indicated conditions and time points post-injury. *B,* representative macroscopic appearance of wounds at indicated time points post-injury; *day 5* post-injury, wounds treated with 2.0 mg/ml rα1-ACT revealed almost complete epithelialization; *day 10* post-injury, almost all wounds treated with both concentrations are closed. *C,* representative H&E staining of wound tissues post-injury; in rα1-ACT treated wounds a highly vascularized and cellular granulation tissue developed that is covered by a hyper-thickened and closed epithelium; in contrast, in control mice scarce granulation tissue developed at wound edges and a thin, not closed, epithelium overlays the massive subcutaneous fat layer; *right panel* depicts magnifications of *rectangles* in *left panel. D–G,* morphometric analysis of wound tissue at different time points post-injury. *D,* area of granulation tissue ($p = 0.01$, control *versus* 2.0 mg/ml rα1-ACT day 5; $p = 0.004$, control *versus* 0.4 mg/ml rα1-ACT day 10; $p = 0.003$, control *versus* 2.0 mg/ml rα1-ACT day 10). *E,* length of epithelial tongue ($p = 0.0001$, control *versus* 2.0 mg/ml rα1-ACT day 5). *F,* distance between epithelial tips ($p = 0.0004$, control *versus* 2.0 mg/ml rα1-ACT day 5). *G,* distance between injured edges of panniculus carnosus ($p = 0.04$, control *versus* 0.4 mg/ml rα1-ACT day 5; $p = 0.0006$, control *versus* 2.0 mg/ml rα1-ACT day 5), at each time point and for each condition, 12 wounds from three different mice were analyzed; *dashed line* indicates granulation tissue; *arrows* indicate tip of epithelial tongue; *arrowheads* indicate ends of the injured panniculus carnosus at the wound edge; *e,* epidermis; *d,* dermis, *gr,* granulation tissue; *sft,* subcutaneous fat tissue. *Scale bar,* 400 μm. *, $p = 0.01$ to 0.05; **, $p = 0.001$ to 0.01; ***, $p < 0.001$.
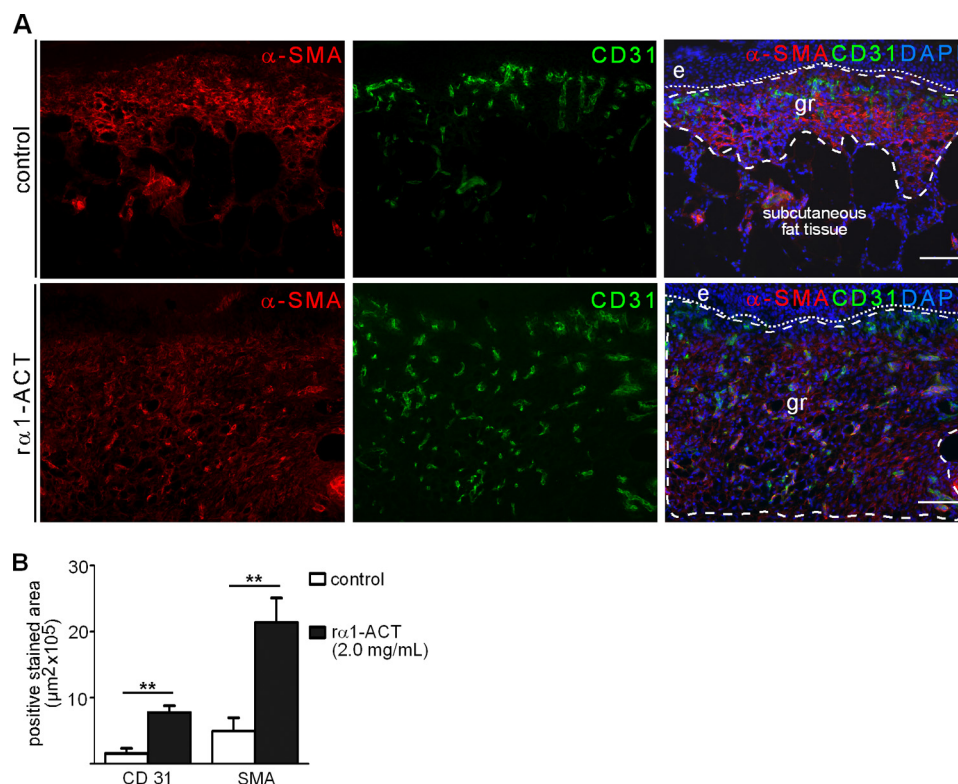
FIGURE 3. **rα1-ACT treatment increases angiogenesis and myofibroblast differentiation in wounds of diabetic mice.** *A,* immunofluorescence staining of cryosections from vehicle-treated (*control*) and rα1-ACT-treated (2 mg/ml) wounds, day 10 post-injury. *B,* morphometric quantification of the area within the granulation tissue that stained positive for α-SMA and CD31, day 10 post-injury (α-SMA, $p = 0.008$, control *versus* 2.0 mg/ml rα1-ACT; CD31, $p = 0.003$, control *versus* 2.0 mg/ml rα1-ACT); for each condition 12 wounds from three different mice were analyzed. *Dashed line* outlines granulation tissue, and *dotted line* indicates the epidermal-dermal junction; *e,* epidermis; *gr,* granulation tissue. *Scale bar,* 100 μm. **, $p = 0.001$ to 0.01.

ulation tissue that had developed beneath the neoepidermis and that extended into deep dermal layers (Fig. 3*A*). The number of α-SMA-positive cells as well as the staining intensity of positive cells was significantly increased in rα1-ACT treated wounds when compared with controls ($p < 0.008$) (Fig. 3*B*), indicating that augmented myofibroblast differentiation was responsible for the enhanced contraction of rα1-ACT-treated wounds.

To determine whether the increased staining for α-SMA in rα1-ACT wounds might be due to an increased number of vascular structures coated with α-SMA-positive perivascular cells, we performed immunofluorescence double labeling for CD31 and α-SMA. At day 10 post-wounding, rα1-ACT-treated wounds showed a highly vascularized granulation tissue, which was significantly increased when compared with vehicle-treated wounds ($p < 0.003$) (Fig. 3*B*). The tissue between capillary structures stained positive for α-SMA, indicating a nonvascular cell origin of this staining and suggesting the presence of myofibroblasts.

Endogenous α1-ACT Activity Is Attenuated in Exudates Obtained from Nonhealing Versus Healing Human Wounds— Our findings in mice revealed a functional link between decreased Spi-2 expression and an impaired healing condition as well as the rescue of this phenotype by locally restoring α1-ACT/Spi-2 activity. We thus investigated the hypothesis that disturbed α1-ACT activity also contributes to human wound healing pathology. We evaluated both the activity and integrity of α1-ACT in exudates obtained from normally heal-

ing and nonhealing chronic human skin wounds (venous ulcers). To quantify the activity of endogenous α1-ACT protein in wound exudates, an *in vitro* substrate-protease binding assay was developed. To this end, α1-ACT activity was determined by assessing the binding capacity of free α1-ACT to cathepsin G. Wound exudate is the interstitial fluid of wounded tissue and contains numerous soluble mediators, extracellular matrix molecules, proteases and their inhibitors, as well as their degradation products. It represents a liquid biopsy that reflects the metabolic condition of the wound and has been proven to be useful in identifying factors involved in skin physiology and pathology (5, 6, 26). Exudate collection and processing followed a standardized protocol. Clinical features characterizing the patients and wounds from which exudates were collected are summarized in supplemental Table 1. Exudates were obtained from patients with normal healing wounds in the lower leg during the phase of granulation tissue formation ($n = 5$, 8–10 days post-injury) and patients presenting with venous ulcers in the nonhealing state for a minimum of 6 months ($n = 15$). Patients were not affected by other diseases that would compromise the regenerative capacity of skin, including arterial disease or diabetes mellitus. In all exudates, the concentration of active α1-ACT was significantly decreased compared with the mean plasma levels of 430 μg/ml, which were within the range of reported values (33). In normal healing wounds, a median concentration of 53 μg/ml active α1-ACT protein ($n = 5$) was detected (Fig. 4*A*). In contrast, activity of endogenous α1-ACT was significantly decreased in exudates derived from nonheal-
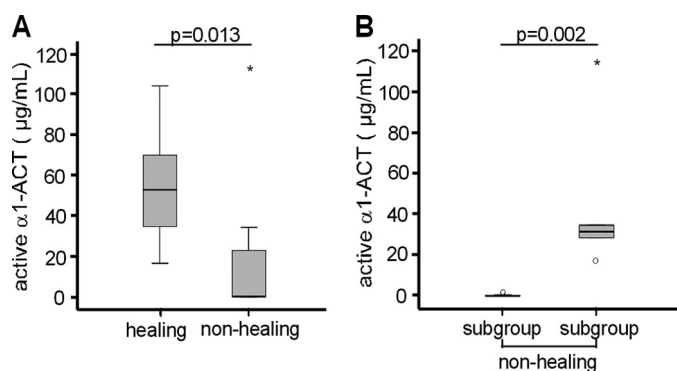
FIGURE 4. **Endogenous, rα1-ACT activity is attenuated in exudates obtained from nonhealing *versus* healing human wounds.** *A,* box plot diagram illustrates activity of α1-ACT protein in exudates obtained from healing (*n* = 5) and nonhealing (*n* = 15) human wounds. *B,* box plot diagram illustrating segregation of exudates obtained from patients with nonhealing wounds in two subgroups, based on endogenous α1-ACT activity levels <1 (*n* = 10) or >1 (*n* = 5) mg/ml; *asterisk* and *circle* illustrate divergent values.

ing wounds (median = 0.36 µg/ml, *p* = 0.013) (Fig. 4*A*). Although the majority of venous ulcer exudates had activity levels below 1 µg/ml (*n* = 10), a small fraction of exudates (*n* = 5) had activity levels similar to healing wounds (Fig. 4*B*). Fig. 4*B* illustrates this segregation of α1-ACT activity levels in two subgroups (based on α1-ACT activity <1 µg/ml (subgroup 1) or higher (subgroup 2)). Overall, these findings demonstrate that in the majority of human chronic venous ulcers, endogenous α1-ACT activity was significantly reduced when compared with healing wounds.

Integrity of rα1-ACT Added into Wound Exudate Correlates Positively with the Activity of Endogenous α1-ACT—To investigate the question whether loss of endogenous α1-ACT activity found in human nonhealing wounds correlated with decreased stability of α1-ACT protein, rα1-ACT was added into wound exudates for defined times, and its integrity was assessed by Western blot analysis. Wound exudates obtained from nonhealing and normal healing wounds, which had not been supplemented with rα1-ACT, all showed an immunoreactive product that migrated with an approximate molecular mass of 50 kDa (Fig. 5*A*). This band had an electrophoretic mobility similar to α1-ACT protein isolated from human plasma. To a various extent, exudates exhibited additional bands with higher molecular masses ranging between ∼50 and 70 kDa. Based on the analysis of rα1-ACT·cathepsin G complexes by reducing SDS-PAGE (supplemental Fig. 1), these bands most likely represented endogenous α1-ACT·substrate complexes that were intact or partially degraded. Incubation of rα1-ACT with wound exudate obtained from nonhealing wounds (Fig. 5*C*), but not from healing wounds (Fig. 5*B*), revealed either protein stability or partial degradation. In three of five exudates obtained from nonhealing wounds (numbers 1, 2, and 4), we detected not only the intact rα1-ACT that migrated at ∼38 kDa but also a smaller protein of ∼34 kDa after a 30-min incubation period (Fig. 5*C*). This band indicated a proteolytic cleavage product of rα1-ACT (rα1-ACT fragment). Prolonged incubation up to 24 h resulted in complete rα1-ACT degradation in two of those three exudates (numbers 1 and 2), as indicated by loss of the 38-kDa band and the appearance of a single prominent band at 34 kDa (Fig. 5*C*). In two exudates
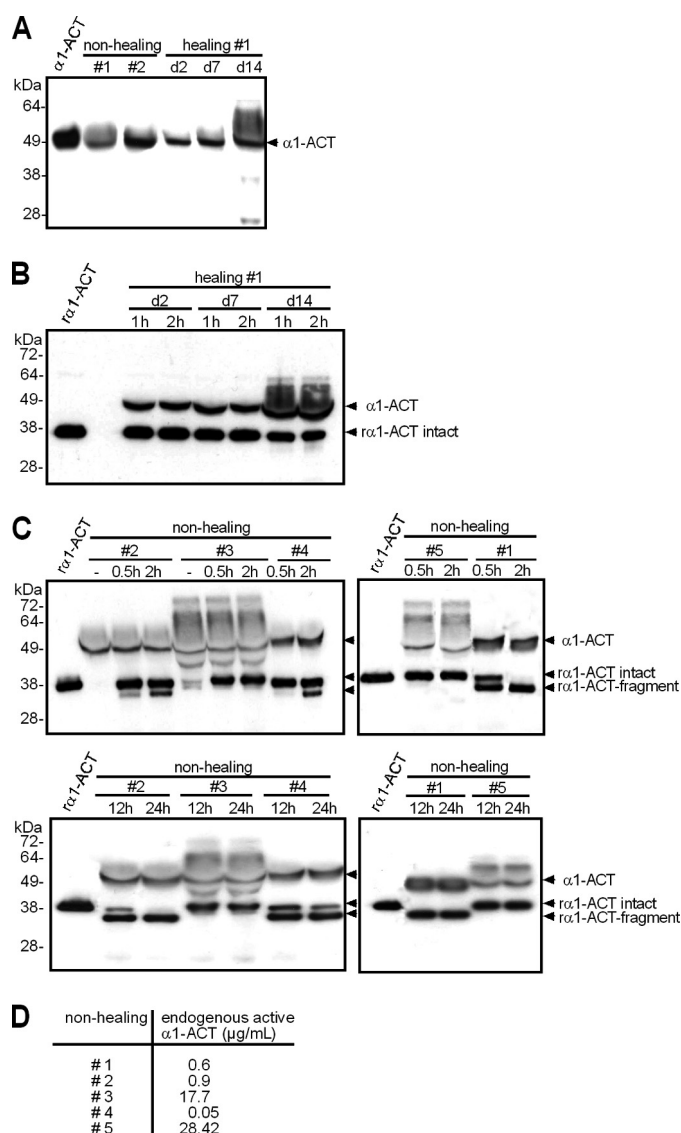

FIGURE 5. **rα1-ACT is a target of wound proteases.** *A–C,* Western blot analysis for α1-ACT; samples were subjected to reducing SDS-PAGE analysis, and integrity of α1-ACT protein was determined by detecting immunoreactive products with an α1-ACT-specific antibody. *A,* human plasma α1-ACT (600 ng/lane); exudates obtained from nonhealing (*#1* and *#2*) or healing (*#1,* postoperative days (*d*) 2, 7, and 14) wounds. *B* and *C,* rα1-ACT (600 ng/lane) was incubated in wound exudates obtained from healing (*B, #1*) or nonhealing (*C, #1–#5*) wounds for time periods as indicated. *Arrowheads* indicate endogenous α1-ACT (*α1-ACT*), intact rα1-ACT (*rα1-ACT intact*), and fragments of rα1-ACT (*rα1-ACT fragment*). *D,* activity of endogenous α1-ACT in exudates obtained from nonhealing wounds (*#1–5*).

obtained from nonhealing wounds (numbers 3 and 5), rα1-ACT remained stable over 24 h of incubation (Fig. 5*C*). Of note, rα1-ACT fragmentation correlated positively with low endogenous α1-ACT activity measured in the majority of exudates derived from nonhealing wounds (Fig. 4*A*), and rα1-ACT stability correlated positively with high levels of endogenous α1-ACT activity, detected in a subgroup of exudates (Fig. 5*D*). These findings indicate that in chronic human wounds proteolytic fragmentation contributes to attenuate activity of endogenous α1-ACT.

Identification of a Novel Proteolytic Cleavage Site of rα1-ACT in Nonhealing Human Wounds—To identify potential sites in the rα1-ACT protein, which are recognized by proteinases
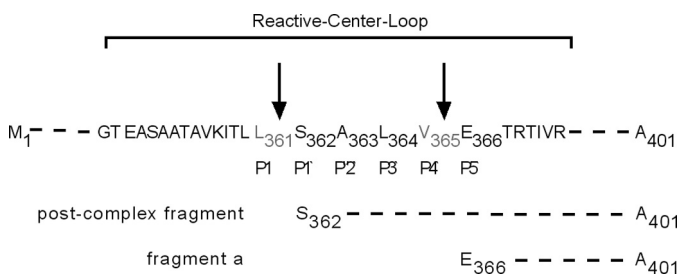
FIGURE 6. **LC-MS analysis of rα1-ACT fragments present in human non-healing wounds.** α1-ACT amino acid sequence of reactive center loop, identified cleavage sites (indicated by *arrow*), and α1-ACT fragments are shown.

FIGURE 7. **Neutrophil elastase inhibitor rescues the stability and activity of rα1-ACT in nonhealing human wounds.** *A,* exudate (*#1*) obtained from a nonhealing wound was incubated with SSR 69071 to reach different final concentrations as indicated and then rα1-ACT was added. At the indicated time points, intact rα1-ACT protein was quantified by LC-MS analysis. *B,* SSR 69071 or PBS (control) was added to exudates obtained from nonhealing wounds (*#1, #5, #11,* and *#12*) and then rα1-ACT was added; after 12 h, rα1-ACT activity was quantified by ELISA.

present in the exudate of nonhealing wounds, rα1-ACT was incubated in exudates, and degradation fragments were characterized by LC-MS analysis. Based on current knowledge, two fundamentally different mechanisms could be responsible for the degradation of α1-ACT in chronic wounds. First is the formation of stoichiometric 1:1 complexes with its target proteinases, and second is cleavage by proteinases that α1-ACT itself is unable to inhibit. Regarding the first mechanism, Nair and Cooperman (21) found that the release of a 4625-Da C-terminal peptide, which includes a part of the reactive center loop of α1-ACT, is the result of the α1-ACT·chymotrypsin complex formation. It was therefore called the post-complex fragment (Fig. 6).

In the chromatogram of exudates obtained from nonhealing wounds (*n* = 5) with addition of rα1-ACT, two fragments were identified with high confidence and incidence as follows: the post-complex fragment (amino acids 362–401) and a more truncated C-terminal fragment that was cleaved between Val-365 and Glu-366, and called fragment "a" (amino acids 366–401) (Fig. 6 and supplemental Fig. 2). For both fragments, the relative deviation between the expected and identified molecular weight was less than 0.008%. Of note, whereas the post-complex fragment was detected with high incidence in exudates characterized by low α1-ACT degrading activity, fragment a was abundantly present in exudates with high α1-ACT degrading activity. Overall, these findings reveal the generation of canonical (caused by proper substrate·protease complex formation) and uncommon cleavage sites within the reactive center loop in the microenvironment of nonhealing human wounds, with each cleavage leading to proteolytic inactivation of α1-ACT.

Neutrophil Elastase Inhibitor Significantly Increases Stability and Activity of rα1-ACT in Exudate Obtained from Nonhealing Human Wounds—To characterize rα1-ACT-degrading proteases present in the microenvironment of nonhealing wounds, rα1-ACT was incubated with wound exudate in the presence of various protease inhibitors. Integrity of rα1-ACT was assessed by LC-MS analysis. Based on the identification of cleavage fragment a, we speculated that neutrophil elastase contributed to α1-ACT fragmentation in chronic human wounds (valine at position P1 and alanine at position P3). To test this hypothesis, we analyzed the ability of SSR 69071, a potent inhibitor of human neutrophil elastase (IC$_{50}$ = 3.9 nmol/liter) (34), to block rα1-ACT fragmentation in wound exudate. Exudates characterized by high rα1-ACT degrading and inactivating activity were incubated with SSR 69071 at different concentrations
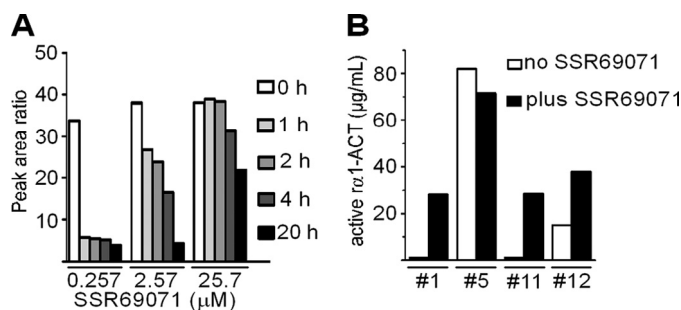
prior to addition of rα1-ACT and for different times as indicated. A clear dose-dependent inhibition of rα1-ACT cleavage was evident (Fig. 7*A*). Furthermore, direct evidence for a role of neutrophil elastase in rα1-ACT cleavage and subsequent loss of activity was provided by partial protection of rα1-ACT activity by preincubation of wound exudates with SSR 69071 (Fig. 7*B*). Several inhibitors of metal-dependent enzymes (*e.g.* matrix metalloproteinases), including ciclopiroxolamin, deferoxamine, phenanthroline, doxycycline, or EDTA had no significant effect on rα1-ACT stabilization in exudates derived from nonhealing wounds, suggesting a minor contribution of matrix metalloproteinase-mediated cleavage (data not shown). Overall, these findings demonstrate a critical role for neutrophil elastase-mediated cleavage and subsequent inactivation of α1-ACT in human nonhealing wounds.

DISCUSSION

Our study provides substantial evidence for an important role of locally acting α1-ACT/Spi-2 in the restoration of skin integrity following injury. By examining human and murine skin wounds, we showed that the physiological repair response is associated with increased α1-ACT/Spi-2 gene expression at the wound site. In both species, attenuated α1-ACT/Spi-2 activity and/or gene expression at the local wound site was associated with severe wound healing defects. Local application of rα1-ACT protein to wounds of diabetic mice rescued the impaired healing phenotype, primarily because of increased granulation tissue deposition and maturation, as well as accelerated epithelialization. Therefore, our study emphasizes a pivotal function of α1-ACT/Spi-2 in wound healing, provides mechanistic insights into its physiological and pathological role in skin repair, and offers perspectives for the development of novel therapeutic strategies for impaired healing conditions.

α1-ACT/Spi-2 Expression Exhibits an Acute Phase Response upon Skin Injury and Might Be Added as a New Member of Skin-derived Serine Proteinase Inhibitors—In mice and humans, the liver synthesis is thought to be the major source of α1-ACT/Spi-2, and α1-ACT/Spi-2 is considered a classical systemic plasma-derived proteinase inhibitor. Therefore, our finding of a dramatic increase of local Spi-2 and α1-ACT expression in skin wounds of wild-type mice and humans during the

inflammatory phase of repair was unexpected. There is evidence for extrahepatic sites of α1-ACT synthesis in lung epithelial cells and in leukocytes (35, 36). Our immunohistochemical findings revealed α1-ACT expression in wounded epidermis and infiltrating leukocytes. In view of its known role as acute phase protein (24), up-regulation of α1-ACT activity immediately after skin injury and its persistence during the phase of inflammation might contribute to the counterbalance of polymorphonuclear leukocyte-derived enzymes at the wound site. Polymorphonuclear leukocytes start to infiltrate the wound site within minutes after injury. To our knowledge, α1-ACT/Spi-2 expression in skin following injury has not been previously reported, and our finding should add α1-ACT as a new member of the skin-derived serine proteinase inhibitors that protect the wound tissue from potent leukocyte-derived enzymes.

rα1-ACT Rescues Impaired Wound Healing in Diabetic Mice and Might Protect Wound Tissue from Damage Mediated by Leukocyte-derived Enzymes—To investigate whether a local deficiency of α1-ACT at the wound site can be rescued by local substitution of α1-ACT, we topically applied rα1-ACT into wounds of diabetic mice and characterized the healing response. The db/db model is widely used as model to study impaired wound healing mechanisms and to validate therapeutic concepts. Epithelialization and development of granulation tissue formation are significantly delayed in excisional wounds in these mice. The underlying pathology is complex; however, a prolonged inflammatory response (27, 30) leading to imbalanced protease/inhibitor equilibrium and tissue destruction is considered a critical pathomechanism. So far, the role of α1-ACT during skin repair in these mice has not been examined. We found that in wounds of db/db mice, Spi-2 expression was significantly reduced when compared with wild-type wounds at all time points analyzed, indicating a disturbed balance between the Spi-2 gene product and its target proteases. Most importantly, in db/db mice repeated topical application of rα1-ACT protein significantly accelerated the kinetics of wound closure and rescued the diabetes-associated delay in wound repair. Increased epithelialization as well as augmented deposition of highly vascularized granulation tissue and wound contraction contributed to the increased healing rate. Whether these biologically complex, vulnerary events are mediated by antiproteinase activity of α1-ACT and/or whether they reflect indirect effects requires further investigation. Various mechanisms can be delineated; a direct inhibitory effect on target proteases is supported by evidence that both neutrophil-derived cathepsin G and chymotrypsin are potent chemoattractants for neutrophils and monocytes (22, 37), and α1-ACT has been shown to inhibit this activity (38). In particular, cathepsin G has emerged as a potent regulator of inflammatory processes because of its role in proteolytic modification of chemokines (22, 39–41), integrin clustering with subsequent cytoskeletal reorganization and chemokine release (42, 43), modulation of proteinase-activated receptor proteins, and binding to the formyl-peptide receptor (44). Therefore, it is reasonable to speculate that rα1-ACT healing-promoting effects might be mediated by inhibition of leukocyte recruitment and subsequent dampening of downstream proinflammatory and tissue-

destructive events. Furthermore, cathepsin G has been shown to be directly involved in the degradation of extracellular matrix molecules that are essential for skin repair, including collagen (45), elastin (46), and fibronectin (47). This degradation might be inhibited by topical rα1-ACT application. Finally, the rα1-ACT·protease complex can effectively inhibit superoxide anion production in activated neutrophils (23), a mechanism that might contribute to inflammation-mediated impaired healing in db/db mice.

Neutrophil Elastase Is Critical for α1-ACT Fragmentation and Inactivation in Nonhealing Human Skin Wounds—Our findings in mice underscore critical functions of local α1-ACT for proper wound healing. This seems also the case for the human situation, as we found high levels of active α1-ACT in exudates obtained from wounds in healthy patients, whereas in the majority of nonhealing wounds active α1-ACT was almost absent. In western countries venous hypertension is the leading cause of impaired healing conditions in man, raising a significant medical and economic burden for the society. To date, no animal model is available that reflects the pathology of venous ulcers. We show that an uncommon proteolytic cleavage site within the reactive center loop plays an important role in exudate-mediated rα1-ACT cleavage and subsequent inactivation. Neutrophil elastase was strongly implicated in this process. To our knowledge, this is the first report of a rare neutrophil elastase-mediated α1-ACT fragmentation and inactivation process in the human system. More than a decade ago, several groups reported on α1-ACT sensitivity to a variety of enzymes, including microbial and mammalian proteinases (48–52). However, most of these studies were performed *in vitro* using highly purified and/or recombinant proteinases. To date, knowledge regarding α1-ACT stability *in vivo*, in particular in clinically relevant conditions, has been missing.

Using LC-MS analysis, two different α1-ACT peptide fragments were identified with high confidence in rα1-ACT-degrading exudates. The post-complex fragment (peptide 362–401) indicates cleavage at position P1/P1′ (Leu-361/Ser-362), and a fragment consisting of amino acids 366–401 indicates cleavage at position P4′/P5′ (Val-365/Glu-366). The post-complex fragment has been identified in earlier *in vitro* studies and results from complex formation of α1-ACT with its known target proteases, hence revealing proper function of α1-ACT (21). This typical fragment was predominantly found in a subset of nonhealing exudates characterized by high activity of endogenous α1-ACT and by a low incidence of uncommon rα1-ACT degradation. These findings indicate, to some extent, proper function of α1-ACT in a minority of nonhealing human wounds. In future studies it will be interesting to determine whether other proteinase inhibitors are affected in this subset of patients.

More importantly, however, identification of the cleavage position P4′/P5′ (Val-365/Glu-366) in the majority of exudates provides strong evidence that neutrophil elastase can override α1-ACT integrity and activity in the chronic wound microenvironment. Several reasons argue for this assumption. First, investigations by several groups identified valine at position P1 as a requirement for cleavage by neutrophil elastase (53, 54), and alanine at position P3 has been shown to be conducive for

neutrophil elastase cleavage (55). Second, the cleavage fragment a (amino acids 366–401) was predominantly detected in exudates characterized by high rα1-ACT degrading activity that was efficiently blocked by a potent inhibitor of neutrophil elastase. Third, many groups including our own, have measured significantly increased levels of neutrophil elastase activity in chronic *versus* healing human wounds (5, 6, 26). Nevertheless, at this stage we cannot rule out that in addition to neutrophil elastase other proteases within wound exudate might contribute to α1-ACT inactivation.

The findings reported here might be of relevance for other chronic inflammatory and tissue-destructive diseases in which the perturbation of the local α1-ACT-target protease equilibrium is the underlying pathological mechanism. For example, inactivation of α1-ACT and dysregulated cathepsin G has been associated with the degradation of articular cartilage proteoglycans in patients with rheumatoid arthritis (56) and lung tissue destruction causing emphysema (57). In the context of chronic inflammatory diseases, therapeutic α1-ACT might protect tissue from undesirable destructive side effects of leukocyte-derived proteases.

REFERENCES

1. Gurtner, G. C., Werner, S., Barrandon, Y., and Longaker, M. T. (2008) *Nature* **453,** 314–321
2. Nathan, C., and Ding, A. (2010) *Cell* **140,** 871–882
3. Zabel, B. A., Zuniga, L., Ohyama, T., Allen, S. J., Cichy, J., Handel, T. M., and Butcher, E. C. (2006) *Exp. Hematol.* **34,** 1021–1032
4. Chen, P., and Parks, W. C. (2009) *J. Cell. Biochem.* **108,** 1233–1243
5. Herrick, S., Ashcroft, G., Ireland, G., Horan, M., McCollum, C., and Ferguson, M. (1997) *Lab. Invest.* **77,** 281–288
6. Buchstein, N., Hoffmann, D., Smola, H., Lang, S., Paulsson, M., Niemann, C., Krieg, T., and Eming, S. A. (2009) *Am. J. Pathol.* **174,** 2116–2128
7. Eming, S. A., Krieg, T., and Davidson, J. M. (2007) *J. Invest. Dermatol.* **127,** 514–525
8. Weiss, S. J., Curnutte, J. T., and Regiani, S. (1986) *J. Immunol.* **136,** 636–641
9. Huttunen, M., and Harvima, I. T. (2005) *Br. J. Dermatol.* **152,** 1149–1160
10. van Bergen, B. H., Andriessen, M. P., Spruijt, K. I., van de Kerkhof, P. C., and Schalkwijk, J. (1996) *Arch. Dermatol. Res.* **288,** 458–462
11. Wingens, M., van Bergen, B. H., Hiemstra, P. S., Meis, J. F., van Vlijmen-Willems, I. M., Zeeuwen, P. L., Mulder, J., Kramps, H. A., van Ruissen, F., and Schalkwijk, J. (1998) *J. Invest. Dermatol.* **111,** 996–1002
12. Ashcroft, G. S., Lei, K., Jin, W., Longenecker, G., Kulkarni, A. B., Greenwell-Wild, T., Hale-Donze, H., McGrady, G., Song, X. Y., and Wahl, S. M. (2000) *Nat. Med.* **6,** 1147–1153
13. Zhu, J., Nathan, C., Jin, W., Sim, D., Ashcroft, G. S., Wahl, S. M., Lacomis, L., Erdjument-Bromage, H., Tempst, P., Wright, C. D., and Ding, A. (2002) *Cell* **111,** 867–878
14. Gooptu, B., and Lomas, D. A. (2009) *Annu. Rev. Biochem.* **78,** 147–176
15. Carrell, R. W., and Lomas, D. A. (2002) *N. Engl. J. Med.* **346,** 45–53
16. Hidvegi, T., Ewing, M., Hale, P., Dippold, C., Beckett, C., Kemp, C., Maurice, N., Mukherjee, A., Goldbach, C., Watkins, S., Michalopoulos, G., and Perlmutter, D. H. (2010) *Science* **329,** 229–232
17. Porcellini, E., Davis, E. J., Chiappelli, M., Ianni, E., Di Stefano, G., Forti, P., Ravaglia, G., and Licastro, F. (2008) *Curr. Pharm. Des.* **14,** 2659–2664
18. Gettins, P. G. (2002) *Chem. Rev.* **102,** 4751–4804
19. Egelund, R., Rodenburg, K. W., Andreasen, P. A., Rasmussen, M. S., Guldberg, R. E., and Petersen, T. E. (1998) *Biochemistry* **37,** 6375–6379
20. Huntington, J. A., Read, R. J., and Carrell, R. W. (2000) *Nature* **407,** 923–926
21. Nair, S. A., and Cooperman, B. S. (1998) *J. Biol. Chem.* **273,** 17459–17462
22. Pham, C. T. (2006) *Nat. Rev. Immunol.* **6,** 541–550
23. Kilpatrick, L., Johnson, J. L., Nickbarg, E. B., Wang, Z. M., Clifford, T. F., Banach, M., Cooperman, B. S., Douglas, S. D., and Rubin, H. (1991) *J. Immunol.* **146,** 2388–2393
24. Baumann, H., and Gauldie, J. (1994) *Immunol. Today* **15,** 74–80
25. Han, Y. P., Yan, C., and Garner, W. L. (2008) *J. Invest. Dermatol.* **128,** 2334–2342
26. Eming, S. A., Koch, M., Krieger, A., Brachvogel, B., Kreft, S., Bruckner-Tuderman, L., Krieg, T., Shannon, J. D., and Fox, J. W. (2010) *J. Proteome Res.* **9,** 4758–4766
27. Roth, D., Piekarek, M., Paulsson, M., Christ, H., Bloch, W., Krieg, T., Davidson, J. M., and Eming, S. A. (2006) *Am. J. Pathol.* **168,** 670–684
28. Thorey, I. S., Roth, J., Regenbogen, J., Halle, J. P., Bittner, M., Vogl, T., Kaesler, S., Bugnon, P., Reitmaier, B., Durka, S., Graf, A., Wöckner, M., Rieger, N., Konstantinow, A., Wolf, E., Goppelt, A., and Werner, S. (2001) *J. Biol. Chem.* **276,** 35818–35825
29. Forsyth, S., Horvath, A., and Coughlin, P. (2003) *Genomics* **81,** 336–345
30. Wetzler, C., Kämpfer, H., Stallmeyer, B., Pfeilschifter, J., and Frank, S. (2000) *J. Invest. Dermatol.* **115,** 245–253
31. Goova, M. T., Li, J., Kislinger, T., Qu, W., Lu, Y., Bucciarelli, L. G., Nowygrod, S., Wolf, B. M., Caliste, X., Yan, S. F., Stern, D. M., and Schmidt, A. M. (2001) *Am. J. Pathol.* **159,** 513–525
32. Takada, S., Tsuda, M., Fujinami, S., Yamamura, M., Mitomi, T., and Katsunuma, T. (1986) *Cancer Res.* **46,** 3688–3691
33. Aronsen, K. F., Ekelund, G., Kindmark, C. O., and Laurell, C. B. (1972) *Scand. J. Clin. Lab. Invest. Suppl.* **124,** 127–136
34. Kapui, Z., Varga, M., Urban-Szabo, K., Mikus, E., Szabo, T., Szeredi, J., Batori, S., Finance, O., and Aranyi, P. (2003) *J. Pharmacol. Exp. Ther.* **305,** 451–459
35. Burnett, D., McGillivray, D. H., and Stockley, R. A. (1984) *Am. Rev. Respir. Dis.* **129,** 473–476
36. Cichy, J., Potempa, J., Chawla, R. K., and Travis, J. (1995) *J. Clin. Invest.* **95,** 2729–2733
37. Chertov, O., Ueda, H., Xu, L. L., Tani, K., Murphy, W. J., Wang, J. M., Howard, O. M., Sayers, T. J., and Oppenheim, J. J. (1997) *J. Exp. Med.* **186,** 739–747
38. Lomas, D. A., Stone, S. R., Llewellyn-Jones, C., Keogan, M. T., Wang, Z. M., Rubin, H., Carrell, R. W., and Stockley, R. A. (1995) *J. Biol. Chem.* **270,** 23437–23443
39. Hazuda, D. J., Strickler, J., Kueppers, F., Simon, P. L., and Young, P. R. (1990) *J. Biol. Chem.* **265,** 6318–6322
40. Berahovich, R. D., Miao, Z., Wang, Y., Premack, B., Howard, M. C., and Schall, T. J. (2005) *J. Immunol.* **174,** 7341–7351
41. Wittamer, V., Bondue, B., Guillabert, A., Vassart, G., Parmentier, M., and Communi, D. (2005) *J. Immunol.* **175,** 487–493
42. Sambrano, G. R., Huang, W., Faruqi, T., Mahrus, S., Craik, C., and Coughlin, S. R. (2000) *J. Biol. Chem.* **275,** 6819–6823
43. Raptis, S. Z., Shapiro, S. D., Simmons, P. M., Cheng, A. M., and Pham, C. T. (2005) *Immunity* **22,** 679–691
44. Sun, R., Iribarren, P., Zhang, N., Zhou, Y., Gong, W., Cho, E. H., Lockett, S., Chertov, O., Bednar, F., Rogers, T. J., Oppenheim, J. J., and Wang, J. M. (2004) *J. Immunol.* **173,** 428–436
45. Capodici, C., and Berg, R. A. (1989) *Inflammation* **13,** 137–145
46. Reilly, C. F., and Travis, J. (1980) *Biophys. Acta* **621,** 147–157
47. Vartio, T., Seppä, H., and Vaheri, A. (1981) *J. Biol. Chem.* **256,** 471–477
48. Desrochers, P. E., Jeffrey, J. J., and Weiss, S. J. (1991) *J. Clin. Invest.* **87,** 2258–2265
49. Mast, A. E., Enghild, J. J., Nagase, H., Suzuki, K., Pizzo, S. V., and Salvesen, G. (1991) *J. Biol. Chem.* **266,** 15810–15816
50. Potempa, J., Fedak, D., Dubin, A., Mast, A., and Travis, J. (1991) *J. Biol. Chem.* **266,** 21482–21487

51. Rubin, H., Plotnick, M., Wang, Z. M., Liu, X., Zhong, Q., Schechter, N. M., and Cooperman, B. S. (1994) *Biochemistry* **33,** 7627–7633

52. Stavridi, E. S., O'Malley, K., Lukacs, C. M., Moore, W. T., Lambris, J. D., Christianson, D. W., Rubin, H., and Cooperman, B. S. (1996) *Biochemistry* **35,** 10608–10615

53. McRae, B., Nakajima, K., Travis, J., and Powers, J. C. (1980) *Biochemistry* **19,** 3973–3978

54. Stein, R. L., Strimpler, A. M., Hori, H., and Powers, J. C. (1987) *Biochemistry* **26,** 1301–1305

55. Malemud, C. J., and Janoff, A. (1975) *Arthritis Rheum.* **18,** 361–368

56. Abbink, J. J., Kamp, A. M., Nuijens, J. H., Swaak, T. J., and Hack, C. E. (1993) *Arthritis Rheum.* **36,** 168–180

57. Faber, J. P., Poller, W., Olek, K., Baumann, U., Carlson, J., Lindmark, B., and Eriksson, S. (1993) *J. Hepatol.* **18,** 313–321

58. Chomczynski, P., and Sacchi, N. (1987) *Anal. Biochem.* **162,** 156–159

59. Laemmli, U. K. (1970) *Nature* **227,** 680–685